Scientia Iranica (2024) 31(20), 1889–1905

Sharif University of Technology
Scientia Iranica
Transactions B: Mechanical Engineering
https://scientiairanica.sharif.edu

Numerical investigation of convective heat transfer and friction factor of laminar airflow in a perforated trapezoid-shaped plate-fin channel in 3 dimensions with geometric analysis (A new achievement)

Morteza Piradl and Seyed Mehdi Pesteei*

Department of Mechanical Engineering, Faculty of Engineering, Urmia University, Urmia, Iran.

Received 6 April 2022; received in revised form 15 September 2023; accepted 27 November 2023

KEYWORDS
Plate-fin heat exchanger;
3-D;
Trapezoid-shaped;
Perforated;
Nusselt number;
Friction factor;
Area goodness factor.

Abstract. The aim of this study is to develop a unique perforated trapezoid-shaped plate-fin channel. So, a numerical simulation is performed on the mentioned plates with different geometries. The laminar airflow ($10 \leq Re \leq 1000$) passes through the inter-fin passages with perforated fins, whose perforations are distributed equally throughout the duct. The effects of corrugation angle (ϕ), cross-section aspect ratio ($\alpha = H/S_{avg}$), and cross-section inclination angle (Ψ) are studied. This study has identified the improved performance of the Nusselt number and the Fanning friction factor (f) in a variety of Reynolds. A quantitative assessment of the improvement is done by measuring the area goodness factor (j/f) compared with a plain flat channel. Based on the results, with increasing ϕ from 30° to 45°, the mentioned channel's performance improves. However, as the angle increases more, performance begins to decrease. The channel's performance improves with increasing α. Also, the performance improves by changing Ψ from 90° to 76.60°. Based on the results, for a perforated case with $\phi = 45°$, $\alpha = 10$, and $\Psi = 90°$ at $Re = 200$, versus the non-perforated fin, f decreases $\sim 9\%$, and j/f increases $\sim 61\%$. Also, for the above-mentioned perforated case, when Ψ is changed from 90° to 76.60°, at $Re = 200$, f decreases $\sim 1.3\%$, and j/f increases $\sim 8.2\%$.

1. Introduction

Plate fin heat exchangers promote the air-side efficiency and compactness of heat exchangers and are therefore more cost effective. Heat exchangers with compact surfaces have primarily developed due to the need for space-saving, light, and economical heat exchangers [1–5]. In the past, aircraft engine turbochargers have been pioneers in this endeavor [6,7]. These heat exchangers

*. *Corresponding author.*
E-mail addresses: mp.fmech@gmail.com (M. Piradl); sm.pesteei@urmia.ac.ir (S.M. Pesteei)

To cite this article:
M. Piradl and S.M. Pesteei "Numerical investigation of convective heat transfer and friction factor of iaminar airflow in a perforated trapezoid-shaped plate-fin channel in 3 dimensions with geometric analysis (A new achievement)", *Scientia Iranica* (2024), **31**(20), pp. 1889–1905
https://doi.org/10.24200/sci.2023.60223.6676

are mainly characterized by extended surfaces or fins, which give a large surface area per unit volume > 700 m^2/m^3 [1].

Passive, active, and compounded are the three categories of heat transfer enhancement technologies developed to date [2,8]. There are no external power requirements for passive enhancement methods, and they are ideal for air conditioning systems, notably when it comes to noise reduction. There are a number of passive heat exchangers that have been further developed and are currently accessible on the market for a variety of uses [1–8]. Many of these heat exchangers have plate-fin designs, that promote convection heat transfer as well as providing heat transfer surface with a greater density. Developed designs (louvered fins, offset-strip fins, wavy and corrugated fins, and perforated fins) provide major improvements in heat and mass transfer with comparably small pressure drop [1–5,9–11]. As part of their enhancement mechanisms, these cores do more than enlarge the surface or extend the fins; they also cause periodic interruptions and boundary layer thinning, as well as swirls and fluid mixings, along with longer residence times [1–5]. increased convection coefficients enable heat exchangers to become more compact (with a greater surface density), allowing them to operate with a significantly smaller approach temperature difference and a reduced weight and size [1–5,12]. A great deal of attention continues to be paid in the literature to 3rd- and 4th-generation enhancement methods that make usage of modified plate fins to achieve significant improvements in convective heat transfer coefficients [11,13].

Several papers provide the most comprehensive database of laminar forced convection in ducts with different cross-sectional shapes, including Shah and Sekulic's article [3], Shah and London's monograph [12], and Shah and Bhatti's review [14]. Through finite-difference simulations, Sadasivam et al. [15] modeled single- and double-trapezoidal (or hexagonal) ducts in a laminar, fully developed flow regime. The thermal boundary conditions H1 and T were both studied. Various duct aspect ratios, as well as four different trapezoidal angles, were used to determine solutions for temperature and velocity variations. By comparing the flow and temperature distributions, and calculating friction factors and Nusselt numbers, they determined the effects of duct geometry and heating/cooling conditions on thermo-hydraulic performance and provided valuable information for design. Petkov et al. [16] investigated the performance features of a fully developed single-phase flow in a series of rectangular, triangular, elliptical, trapezoidal, and hexagonal tubes using the Extensive Performance Evaluation Criteria (ExPEC). As thermal boundary conditions, constant wall temperatures were selected. It was found that rectangular, trapezoidal, and hexagonal duct layouts outperformed circular tube layouts sometimes. In another work, Reis et al. [17] provided an approximate method of determining the friction factor for rectangular, triangular, and trapezoidal ducts. Four distinct approximation scenarios were analyzed. Through the application of all four approximations, ducts with trapezoidal cross-sections were analyzed for a variety of aspect ratios and trapezoid angles. Their investigation was concentrated on the friction factor dependence on the trapezoid angle for various aspect ratios. In a numerical study, Abed AlKareem et al. [18] evaluated the impact of geometrical and boundary conditions on turbulent airflow and heat transfer behavior in a trapezoidal duct. A number of cases were examined to determine how the heating side affected the Nusselt number and friction factor. Heat transfer properties were analyzed under conditions of constant heat flux (8000 W/m^2) and airflow velocity of 2.5 m/s (Reynolds number of 4200). It was found that the Reynolds number and the shape of the duct had a significant impact on the average Nusselt number and friction factor.

Perforations incorporated into a symmetric wavy plate-fin geometry is a rather new method of passively enhancing heat transfer. Fujii et al. [19,20] presented perhaps the first experimental evidence in this field. Perforated fin cores feature diverging-convergent plates that are trapezoid-shaped and it has been recommended that heat transfer is improved due to secondary flow created by fin transpiration (Injection of fluid into and suction from adjacent flow streams). It was reported by Fujii et al. [19,20] that this kind of fin core possesses the unparalleled performance characteristics of an increase in heat transfer of $\sim$ 50% combined with a reduction of $\sim$ 20% in friction factor. A reduction in friction loss is unusual since an increase in convective heat transfer is generally associated with a pressure drop penalty [2,4]. In light of this, it is worth investigating further. An investigation by Ji et al. [21] evaluated the heat resistance of triangular folded fin heat sinks. These fins were extruded plate fins, slit folded fins, perforated folded fins, and perforated slit folded fins, and each was tested for the similar boundary conditions, namely heat flux, airflow velocity, and air temperature. Based on the experimental results, the triangular folded fins appeared to have a superior thermal resistance compared to the traditional plate fins. For use in particularly powerful electronic devices, slit folded fins and perforated slit folded fins were the most effective. Compared to usual plate-fin heat sinks operating at the same power level, the slit folded fin and the perforated slit folded fin showed approximately 18% and 20% lesser thermal resistance. As well as the increasing fin height, the number of slits in the perforated slit folded fin, reducing fin pitch, and the Reynolds number

had a major impact on cooling performance. A study carried out by Ganorkar and Kriplani [22] examined the effectiveness of perforated fins with lateral circular holes placed in a rectangular duct and evaluated by means of passive heat transfer enhancement. There were different kinds of perforated fins used in the rectangular channel. Different Reynolds numbers were studied in a rectangular channel with perforated fins. In parallel, the convective heat transfer coefficient and the Nusselt number were additionally examined. Based on the results of the experiments, the ratio of the Nusselt number of the perforated fin to the Nusselt number of the non-perforated fin increased with increasing Reynolds number, diameter, and number of holes. The advantage of increasing the diameter and number of the holes was that the fin's weight was reduced. Shahdad and Fazelpour [23] used Fluent software to investigate the flow field and turbulent flow heat transfer between an array of perforated and plain fins at Reynolds numbers in the range of $20000-50000$. During the study, the $k-\varepsilon$ RNG turbulence model and SIMPLE algorithms were used to solve equations of three-dimensional, steady, and incompressible flow of turbulent fluid. They used air with constant physical properties as the working fluid for the simulation. Results of the study showed that perforated fins increased both the convective heat transfer coefficient and the Nusselt number. Two square holes perforated fins demonstrated the best heat transfer coefficient and Nusselt number. Furthermore, the Nusselt number and heat transfer coefficient were found to increase significantly in an increase in Reynolds number. It was found that the pressure on plain fins decreased after they were converted to perforated fins. Because the flow passed between the fins, and, consequently, the drag force exerted on them decreased. By adding some pins to the basic fins along the moving flow, the pressure was reduced, but the heat transfer was greatly increased. In addition, the weight and price of the fins were reduced. Mohammad et al. [24] conducted an experimental study involving the measurement of the forced convection heat transfer characteristics of various perforations consist of rectangular, triangular, and circular perforations as a function of the power input (100 W and 150 W) and various velocities to ascertain the specific perforation shapes needed for the best performance for plate fin heat sinks. It was noticed that the perforation helped to dissipate heat more quickly at the solid/fluid interface in the fin. Turbulence intensity was also increased by the narrow edge of the perforated area. Additionally, they reported that the triangular perforation increased heat transfer coefficient for different power inputs more than circular perforations, rectangular perforations, or no perforations. An experiment by Kumar et al. [25] was conducted to compare the efficiency of a heat exchanger tube equipped with perforated twisted tape insertions with single and double V cuts. At various twist ratios of twisted tape in Reynolds number from 2000 to 25000, the experiments were conducted to determine friction factor and Nusselt number. Using perforated twisted tape inserts, two types of V cuts were applied in order to determine the improvement in thermo-hydraulic efficiencies. With a twist ratio of 2 and perforated twisted tape insertions with double V cuts, the highest thermo-hydraulic efficiency was determined to be 1.69. Noorbakhsh et al. [26] conducted a numerical study to investigate how adding hollow on twisted tape with different aspect ratios can affect the performance of double-pipe heat exchangers. With Reynolds numbers from 3343 to 5496, the water on both sides was numerically analyzed. The evaluation of the results was made by calculating both sides' outlet temperatures, pressure drop, Nusselt number, and efficiency coefficient. The aspect ratios analyzed were 2.25, 1, and 0.44. Based on the findings, forming hollows on twisted tape with $AR = 1$ could result in a higher coefficient of performance. Moreover, the Nusselt number was minimal in the non-hollow model, while the $AR = 1$ model had the highest Nusselt number. In their experiment, Pradeep et al. [27] investigated the natural convection heat transfer in rectangular fin plates without perforations, with square perforations, with triangular perforations, and with circular perforations. In the study, different fins embedded with different types of perforations were compared in order to assess heat transfer rate. It was also shown that perforations, especially those with a high number, caused increased heat transfer areas and decreased temperature differential between the base and tip of the fins. The perforations acted like cavities and confined the flow within them. In the case of perforated fins, the fin's weight was significantly decreased. The heat sink's heat coefficient increased by $35.82-51.29\%$ using perforation in the fins depending on the geometry and shape of the perforations. In an experiment, Srivastava et al. [28] looked at the performance of conical pieces with and without holes in a divergent layout within a heat exchanger tube. The effect of pitch ratio, as well as the location and number of perforations on fluid and thermal characteristics were investigated. Using the inserts, researchers found that the lower-temperature fluid near the middle of the test configuration was successfully mixed with the higher-temperature fluid close to the surface. Reduced frictional losses were a principal benefit of perforated inserts, which also improved thermal and fluid interactions. In addition to decreasing friction factor, the perforations on the smaller base of the conical insert enhanced heat transfer close to the surface. The hydraulic and thermal efficiencies of rectangular finned-tube heat exchangers without and with diamond and circular perforations were evaluated using a numerical-

experimental approach by Rauber et al. [29]. The 3-D turbulent airflow was solved using ANSYS-Fluent package based on the RANS model. The size and shape of fin perforations were investigated using parametric analysis to determine how they affect flow dynamics and heat transfer. It became concluded that large fin perforations would improve the performance and the thermal efficiency of the heat exchanger. In a numerical study, Piradl and Pesteei [30] investigated the characteristics of forced convection for laminar flow regimes ($10 \leq Re \leq 1000$) for periodically fully developed incompressible airflow in perforated trapezoidal-corrugated 2-D plate-fin channels. The influence of the duct geometry was studied. Comparatively to non-perforated channels, the fin surface's porosity displayed the uncommon behavior of increasing heat transfer coefficients while reducing friction factors. Area goodness factor increased about 72%, while friction factor decreased about 11%. Chen et al. [31] developed an efficient intelligent optimization method that uses the Bayesian Optimization algorithm to determine the optimal structure of a Sinusoidal Wavy Plate-Fin Heat Sink With Crosscut (SWHS-WC). Heat transfer and pressure drop were linked to the comprehensive Thermal Performance Factor (TPF), which was the objective function. Three geometric parameters, which included the fin amplitude, period, and phase shift angle of the heat sink, were optimized by integrating parametric modeling, meshing, and numerical computation. The optimized sinusoidal wavy plate-fin heat sink with crosscut had a 17.6% increase in thermal performance compared to the original geometry. This was due to a significant decrease in pressure drop, which could be attributed to the reduction in the synergy angle between the velocity and the pressure gradient. Towsyfyan et al. [32] performed an efficient thermal plan of a plate-fin heat sink with symmetrical semicircular hollow fins vertically organized and exposed to a parallel stream. In order to compare the thermal performance of the different possible designs, i.e., various values for the inner and outer diameters of the perforated fins, a Computational Fluid Dynamics (CFD) investigation was carried out. Additionally, the CFD analysis was carried out on the impact of the pin's pitch on the thermal performance of the studied heat sinks to discover the most efficient layout. The results showed that the base temperature and thermal resistance of the new design were lower, but the Nussult number was higher than the previous studies. Consequently, it could be concluded that the proposed model had a better thermal efficiency in comparison with the previous designs. The impact of Perforated Baffles (PB) on the local Nusselt number and thermo-hydraulic behaviors usage of a thermochromic liquid crystal sheet was completely investigated by Eiamsa-ard et al. [33]. The PB were modeled in two shapes: PB and Perforated Baffle With Square Wings (SW-PBs). Transverse solid baffles (TBs) were also investigated for evaluation. Experimental findings indicated that SW-PBs provided higher Nu than PBs. In addition, it was observed that PBs and SW-PBs resulted in a lower pressure drop than TBs by about 20.49% and 13.98%, respectively. The decrease in friction factor was mainly due to the baffle perforation. Also, the PBs provided TPF up to 1.01 in the least Reynolds number (6000).

The main purpose of this paper is to introduce a new model of finned surfaces in order to increase heat transfer while reducing pressure drop in trapezoidal channels. To achieve this goal, in the continuation of the previous work, a perforated trapezoid-shaped 3-D fin core is modeled and the flow structure and heat transfer characteristics are investigated by changing the duct geometry in the laminar flow regime. The superiority of the new model over the non-perforated trapezoidal channel is examined by considering the geometrically influential parameters. A very attractive feature of the new model is that the addition of perforations results in a substantial reduction in the frontal area and volume of the compact heat exchanger, relative to the plain or non-perforated channel, which is associated with a decrease in friction losses as well as an increase in heat transfer.

2. Simulation of the computations

Figure 1 illustrates the computer modeling of perforated trapezoid-shaped plate-fin heat exchangers in the current work; Assuming constant wall temperature, rates of airflow ($Pr = 0.71$) are considered in laminar regime ($10 \leq Re \leq 1000$). A parametric computational analysis is performed for constant perforations in fin walls (10% of the total area is perforated), modelled as thin slots of the same size with uniform spacing. In order to determine an optimal geometric configuration, the effect of duct geometry, including corrugation angle (ϕ), cross-section aspect ratio ($\alpha = H/S_{avg}$) and cross-section inclination angle (Ψ) , on the thermo-hydraulic performance of the perforated duct is parametrically explored.

2.1. Mathematical simulations

The schematic diagram depicting the geometries of a trapezoid-shaped plate-fin duct is shown in Figure 1(d). The figure shows that the expansion section has an S_1 spacing between plates, whereas the contraction section has an S_2 spacing. The corrugation angle is given by (ϕ), the cross-section aspect ratio is defined as ($\alpha = H/S_{avg}$) and the cross-section inclination angle is given by (Ψ) . A steady, periodically fully developed, constant property, incompressible, laminar airflow ($Pr = 0.71$) with heat exchange (resulting from a constant wall temperature) is assumed. Following

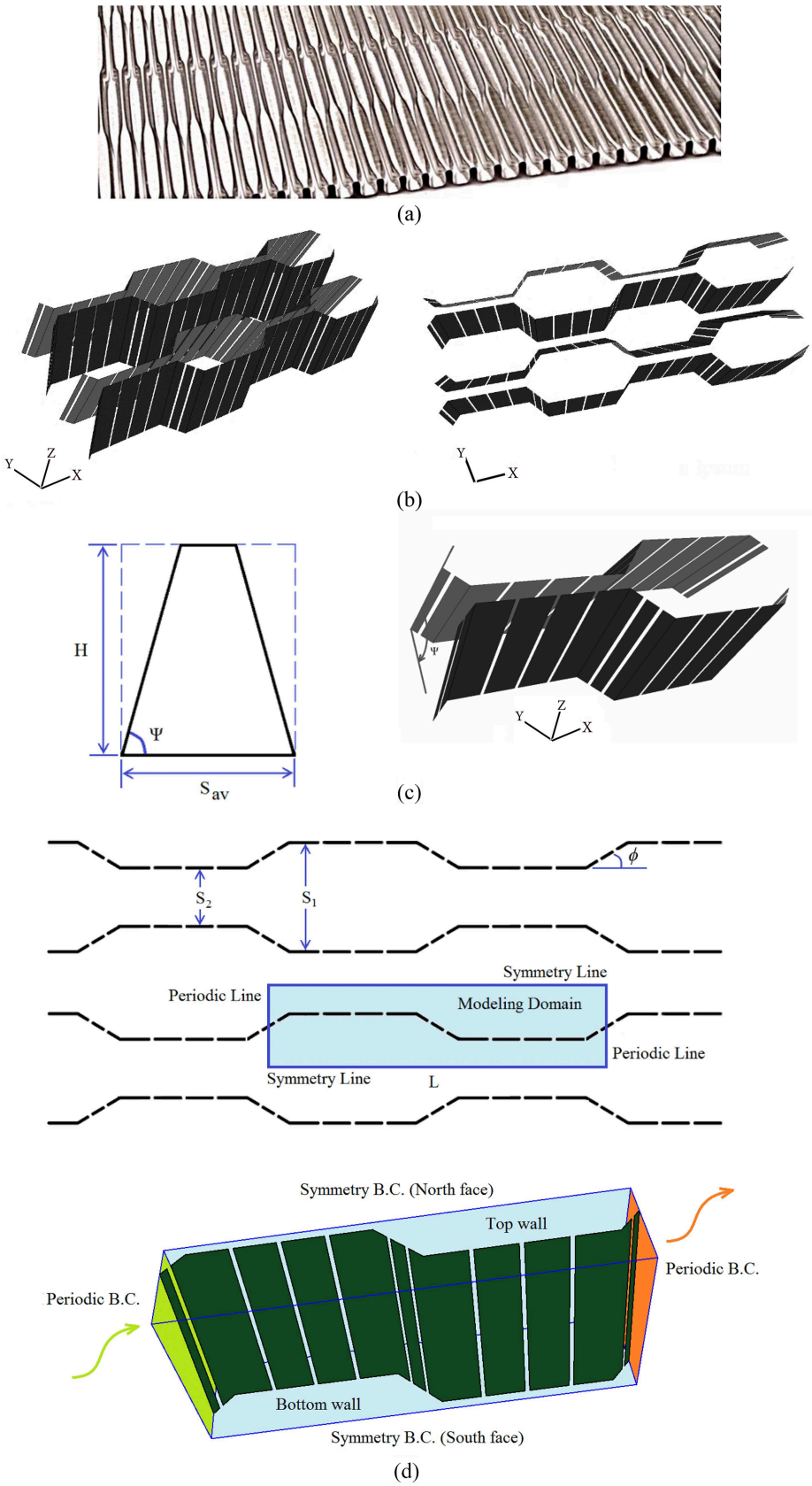

Figure 1. (a) Trapezoidal converging-diverging plate fins; (b) 3-D pattern of the perforated trapezoid-shaped fins; (c) Geometric characteristics of the channel cross section; (d) 2-D and 3-D of modelling domains of perforated trapezoid-shaped plate-fin duct.

are the governing equations for conservation of mass, momentum, and energy:

$$\frac{\partial u}{\partial x}+\frac{\partial v}{\partial y}+\frac{\partial w}{\partial z}=0, \tag{1}$$

$$u\frac{\partial u}{\partial x}+v\frac{\partial u}{\partial y}+w\frac{\partial u}{\partial z}=-\frac{\partial P}{\partial x}+\nu\left(\frac{\partial^2 u}{\partial x^2}+\frac{\partial^2 u}{\partial y^2}+\frac{\partial^2 u}{\partial z^2}\right), \tag{2a}$$

$$u\frac{\partial v}{\partial x}+v\frac{\partial v}{\partial y}+w\frac{\partial v}{\partial z}=-\frac{\partial P}{\partial y}+\nu\left(\frac{\partial^2 v}{\partial x^2}+\frac{\partial^2 v}{\partial y^2}+\frac{\partial^2 v}{\partial z^2}\right), \tag{2b}$$

$$u\frac{\partial w}{\partial x}+v\frac{\partial w}{\partial y}+w\frac{\partial w}{\partial z}=-\frac{\partial P}{\partial z}+\nu\left(\frac{\partial^2 w}{\partial x^2}+\frac{\partial^2 w}{\partial y^2}+\frac{\partial^2 w}{\partial z^2}\right), \tag{2c}$$

$$u\frac{\partial T}{\partial x}+v\frac{\partial T}{\partial y}+w\frac{\partial T}{\partial z}=\alpha\left(\frac{\partial^2 T}{\partial x^2}+\frac{\partial^2 T}{\partial y^2}+\frac{\partial^2 T}{\partial z^2}\right). \tag{3}$$

At the fin walls, as well as at the beginning and end of each period, there are the following boundary conditions:

$$u=v=w=0 \qquad \text{at fin walls}, \tag{4a}$$

$$\frac{u|_{(x=0,y,z)}}{u_b|_{(x=0)}}=\frac{u|_{(x=L,y,z)}}{u_b|_{(x=L)}}, \tag{4b}$$

$$T_w=\text{constan } t, \tag{5a}$$

$$\frac{T|_{(x=0,y,z)}}{T_b|_{(x=0)}}=\frac{T|_{(x=L,y,z)}}{T_b|_{(x=L)}}. \tag{5b}$$

The bulk velocity u_b is expressed as:

$$u_b=\frac{\dot{m}}{\rho A_c}. \tag{6}$$

The Reynolds number can then be obtained by:

$$Re=\frac{\rho u_b D_h}{\mu}. \tag{7}$$

In each period length of the channel, the average pressure loss caused by friction or wall shear stress (τ_{xy}) is described by the Fanning friction factor:

$$f=\frac{\tau_{xy}}{\frac{1}{2}\rho u_b^2}. \tag{8}$$

Additionally, the local bulk temperature ($T_{b,x}$) is described as:

$$T_{b,x}=\frac{1}{u_b A_c}\int u_x T_x dA_c. \tag{9}$$

Taking the local heat transfer coefficient into account, the local Nusselt number can be expressed as follows:

$$Nu_x=\frac{q'' D_h}{k\left(T_{w,x}-T_{b,x}\right)}. \tag{10}$$

Therefore, the average Nusselt number is determined by integrating the local values into the following form:

$$Nu=\frac{1}{L}\int_0^L Nu_x dx. \tag{11}$$

The Colburn j factor, applied mostly in compact heat exchanger design, is described as follows:

$$j=\frac{Nu}{Re.Pr^{1/3}}. \tag{12}$$

In evaluating the velocity and temperature solutions, the following convergence criterion is applied:

$$Error=\left|\left(\Phi^n-\Phi^{n-1}\right)/\Phi^n\right|\leq 10^{-7}. \tag{13}$$

Table 1 summarizes the geometric specifications of the different plate-fins considered for the numerical study. In every case, 10% porosity is applied.

2.2. Numerical procedure

Solution of Eq. (1) through Eq. (3) is numerically performed utilizing standard finite volume methods which employ power-law schemes for energy and flow. The generated mesh during a particular period in the channel is a non-orthogonal grid evenly spaced in the x-direction, somewhat compact in the porous zone, and non-uniform in the y- and z-directions (so the mesh around the fin walls is denser). See Figure 2 for an example grid structure.

Table 1. Geometric specifications of the plate-fin channel (for S_2/S_1=0.36).

Case	Corrugation angle (ϕ)	Cross-section aspect ratio (α=H/S_{avg})	Cross-section inclination angle (Ψ)
1	30°	10	90°
2	45°	10	90°
3	60°	10	90°
4	45°	4	90°
5	45°	2	90°
6	45°	1	90°
7	45°	2	85.46°
8	45°	2	80.98°
9	45°	2	76.60°

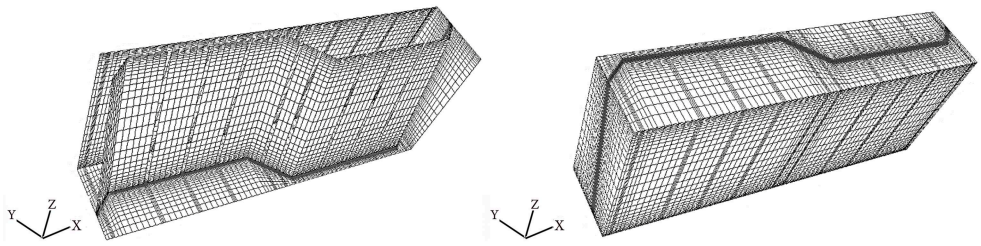

Figure 2. Mesh pattern of 3-D perforated wavy plate-fin channels with trapezoidal profiles.

Table 2. Dimensions of the mesh.

Various grids	φ_h	$\varphi_{2h}{}^*$	φ_{4h}	φ_{8h}	φ_{16h}
X-direction cells number	144	72	36	18	9
Y-direction cells number	64	32	16	8	4
Z-direction cells number	200	100	50	25	12
Number of cells in total	1,843,200	230,400	28,800	3,600	432

2.3. Grid sensitivity analysis

To perform a grid sensitivity analysis, the Nusselt numbers are compared for various grid dimensions of a modeled non-perforated straight plate-fin channel with $\alpha = 10$, and $\Psi = 90°$at $Re = 400$. The simulation grid initially consisted of 230,400 cells. One finer grid and a number of coarser grids were chosen. Table 2 contains details about the various meshes.

The discretization error for a grid can be determined by Ferziger and Peric [34] as follows:

$$\varepsilon_h^d \approx \frac{\varphi_h - \varphi_{2h}}{2^a - 1}, \tag{14}$$

"a" is the scheme's order and is represented by:

$$a = \frac{\log\left(\frac{\varphi_{2h} - \varphi_{4h}}{\varphi_h - \varphi_{2h}}\right)}{\log(2)}, \tag{15}$$

"2" indicates the increase in the mesh dimension in both equations. Based on Eq. (15), at least three meshes are necessary to calculate the discretization error. Errors in calculation due to the logarithm of a negative number can be avoided by ensuring that the three solutions are monotonically convergent. In accordance with Richardson Extrapolation theory [35,36], the finest mesh solution can be added to the discretization error given by Eq. (14) to obtain an approximate grid-independent result. The equation is as follows:

$$\Phi = \varphi_h + \varepsilon_h^d. \tag{16}$$

The grid sensitivity analysis results are displayed in Table 3 along with its plotted results in Figure 3.

As a result, the Nusselt number computed based on these results is in good agreement with analytical values reported in literature [14].

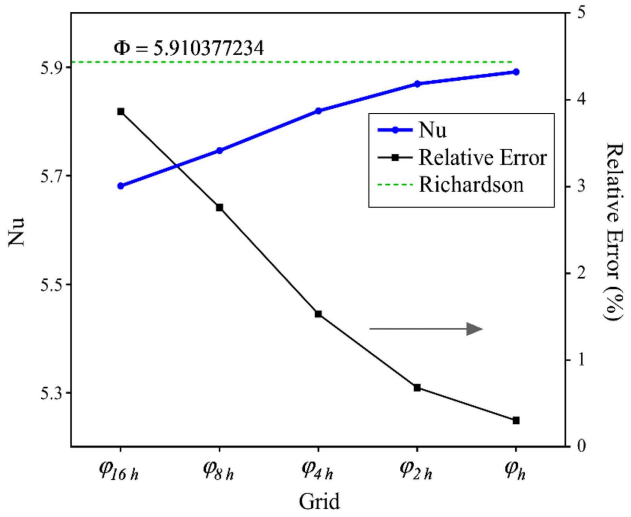

Figure 3. Grid sensitivity analysis of the Nusselt number, with Richardson solution.

2.4. Computational validation

The numerical findings were validated by comparing them with analytical results provided by Shah and London [12] for a 2-D straight parallel plate channel ($\alpha \rightarrow \infty$) and with those provided by Shah and

Table 3. Grid sensitivity analysis results.

The scheme's order (a)	Discretization error ($\varepsilon_h{}^d$)	Finest mesh solution (φ_h)	Richardson solution (Φ)	Analytical solution [14] (Nu)
1.161378102	0.01809501	5.892282224	5.910377234	5.910980575

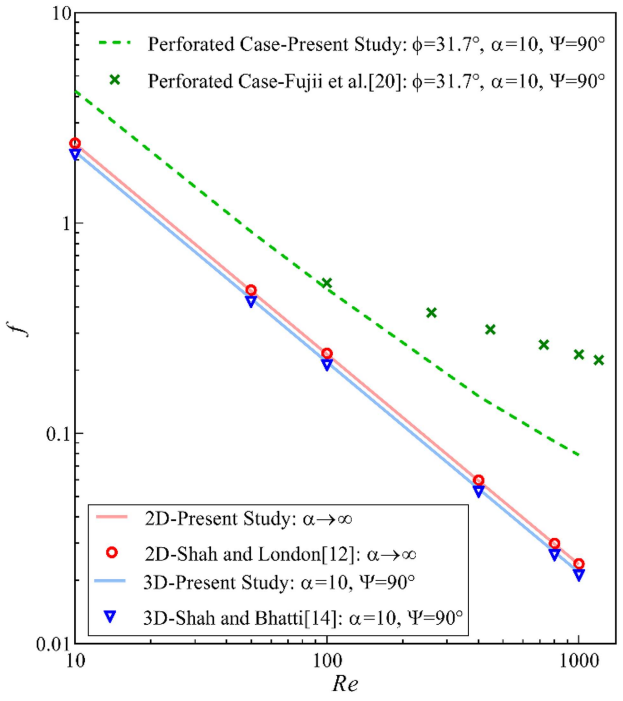

Figure 4. Flow validation, f vs. Re, for selected models and comparison to existing literature.

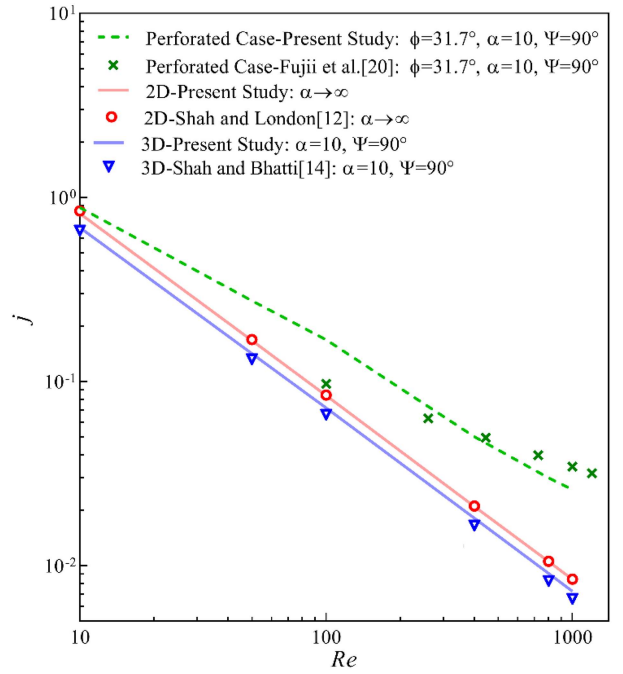

Figure 5. Thermal validation, j vs. Re, for selected models and comparison to existing literature.

Bhatti [14] for a 3-D straight parallel plate channel with a rectangular cross-section ($\alpha = 10$, $\Psi = 90°$). Both the Fanning friction factor and Colburn j factor presented in Figures 4 and 5, respectively, displayed remarkably good agreement for the full Reynolds number range tested. The f-Re and j-Re relations in both figures have a log-linear distribution, and the values of f and j decrease as Re increases. Furthermore, the numerical results of the perforated converging-diverging model with geometrical characteristics of $\phi = 31.7°$, $\alpha = 10$, and $\Psi = 90°$ were compared to the experimental results obtained by Fujii et al. [20] (Figures 4 and 5). The results of the present study differ considerably from Fujii et al.'s in terms of f. It could be the result of an experimental error or the flow may not have developed fully in the computation area.

3. Results and discussion

3.1. The distribution of temperature and flow

The general features of a periodic fully developed fluid flow (air, $Pr = 0.71$) and the thermal fields within middle plane of a usual 3-D converging-diverging plate-fin duct with $\phi = 45°$, $\alpha = 10$ and $\Psi = 90°$ (Figure 6), including fins with and without perforations, are respectively depicted in Figures 7 and 8.

Increasing the flow rate or Re results in the growth of a recirculating zone in the non-perforated plate-fin channel, as indicated in Figure 7(a). Separation of flow is evident at $Re = 100$. Thus, the impact of the thermal boundary layer adjacent to the upstream inclined zone is minimized, as illustrated in Figure 8(a) with $Re = 10$ and 100. Convective heat transfer increases at the converging part of the channel due to this behavior together with an acceleration of the flow in this region. As shown in Figure 7(b), the perforations on the fin surface allow air to flow through it, which breaks up stagnation and recirculation regions, and result in significant fluid mixing cross-fin. By decreasing the fin material, or blocking element, the friction factor is decreased as compared to the non-perforated fins. Furthermore, a perforated or slotted fin surface and the consequent fluid injection and/or blowing, more disrupt the boundary layer, that makes convection heat transfer significantly greater. Figure 8(b) illustrates this. Also, it is seen that the thermal boundary layer becomes considerably thinner as Reynolds increases, resulting in increased heat transfer.

3.2. Effects of geometry

3.2.1. Effect of the corrugation angle (ϕ)

The effect of corrugation angle on temperature distribution as well as flow stream function within middle plane of a 3-D perforated converging-diverging plate-fin channel with $\alpha = 10$, $\Psi = 90°$ (Figure 6(b)) is illustrated in Figure 9 for $Re = 400$. Comparison of flow at $\phi = 30°$ vs $\phi = 60°$ shows that the wedge is more of a barrier in the latter, whereas in the former, the wedge is smoother and bigger. So, this leads to an increase in the fluid velocity and friction factor. The details of the impact of these changes will be presented in the next paragraph.

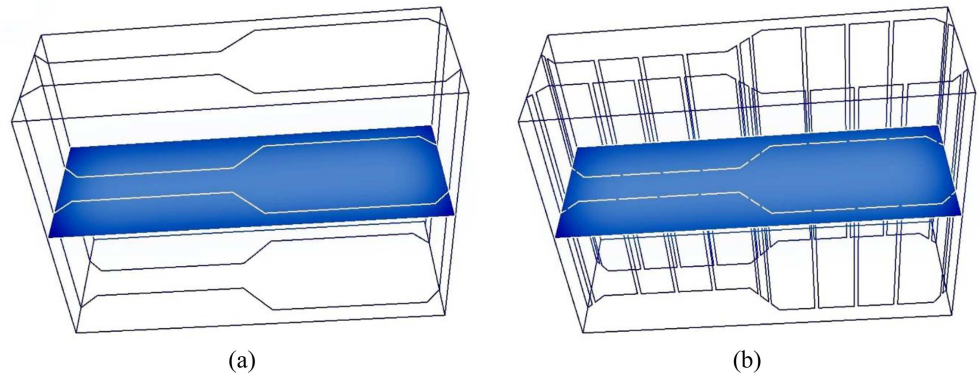

Figure 6. Selected section of the plate-fin channel including trapezoid-shaped fins with $\phi = 45°$, $\alpha = 10$ and $\Psi = 90°$: (a) without perforations and (b) with perforations.

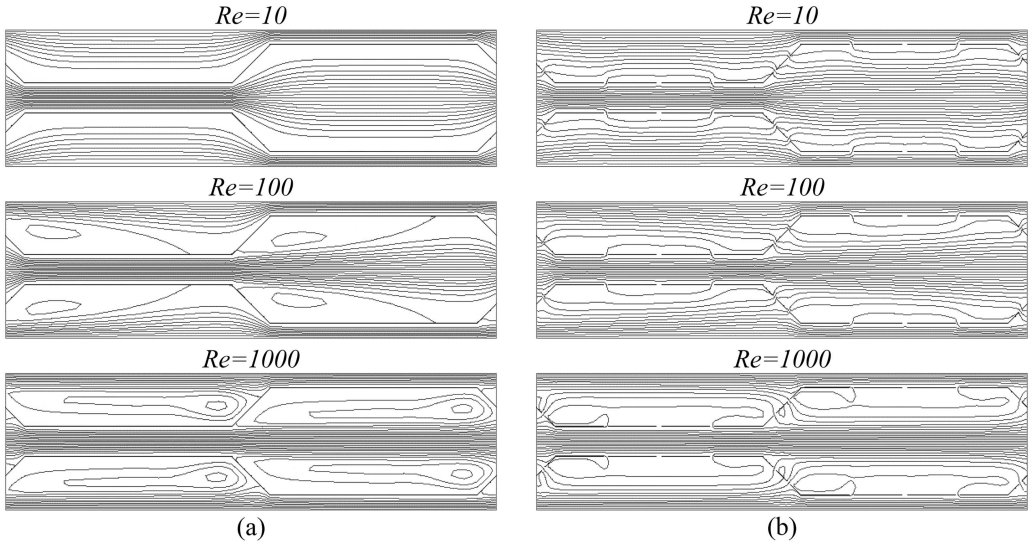

Figure 7. Streamlines for (a) non-perforated, (b) perforated plate-fin channel with $\phi = 45°$, $\alpha = 10$, and $\Psi = 90°$.

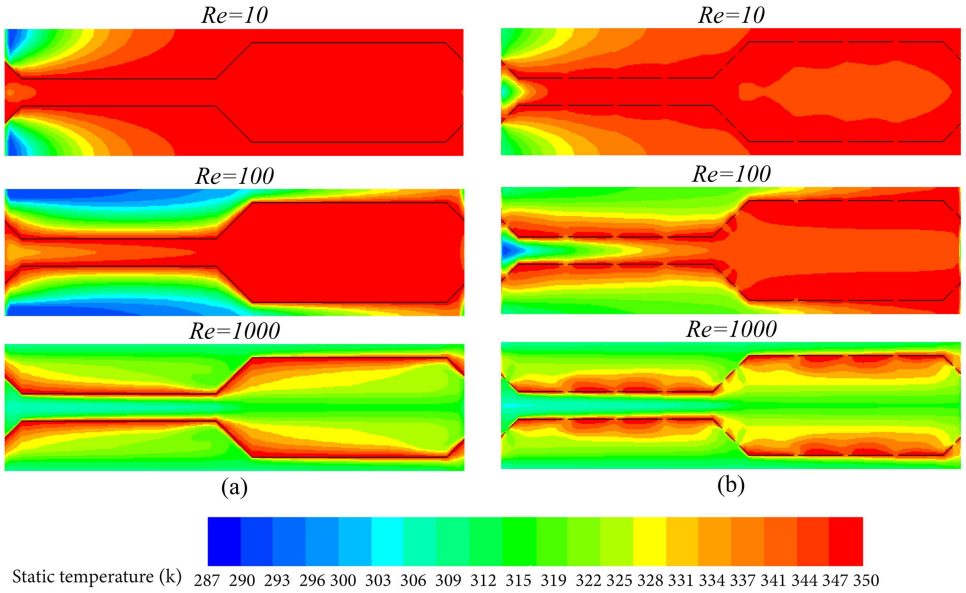

Figure 8. Temperature distribution for (a) non-perforated, (b) perforated plate-fin channel with $\phi = 45°$, $\alpha = 10$, and $\Psi = 90°$.

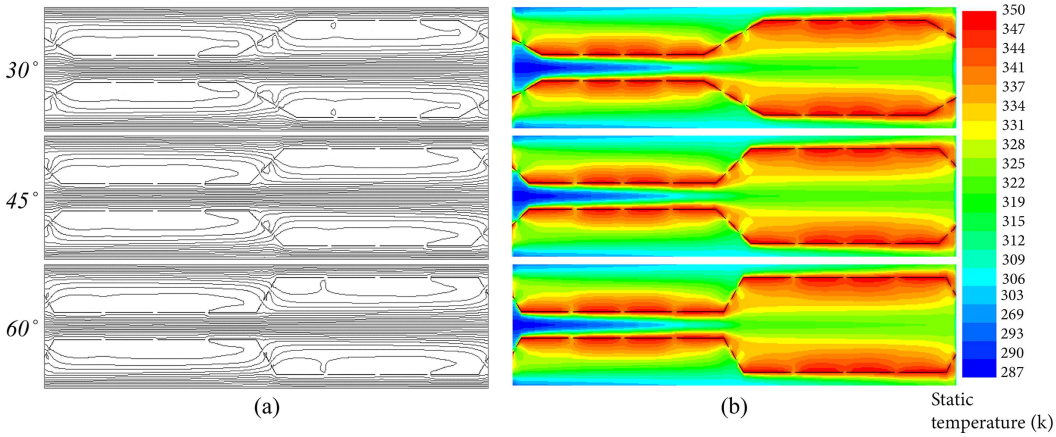

Figure 9. Effect of the corrugation angle (ϕ) on (a) flow streamlines and (b) temperature distribution for a perforated plate-fin channel with $\alpha = 10$, $\Psi = 90°$ at $Re = 400$.

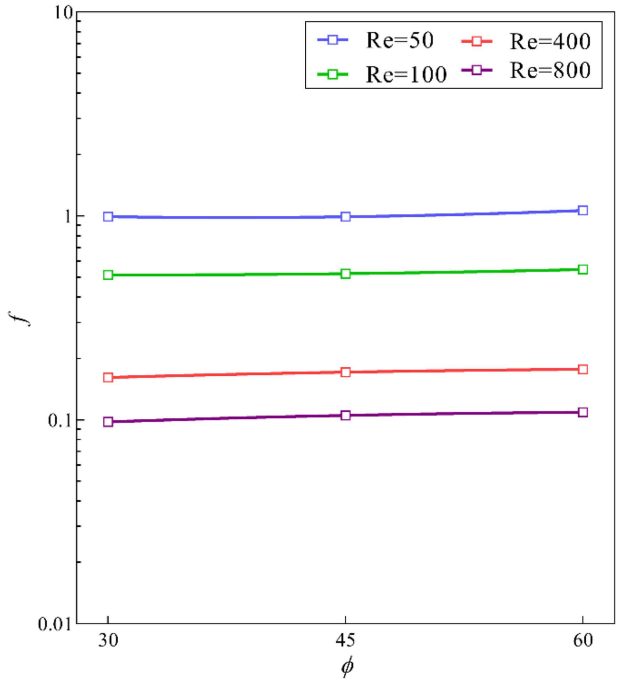

Figure 10. Effects of the change of ϕ on f, for a perforated plate-fin channel with $\alpha = 10$ and $\Psi = 90°$.

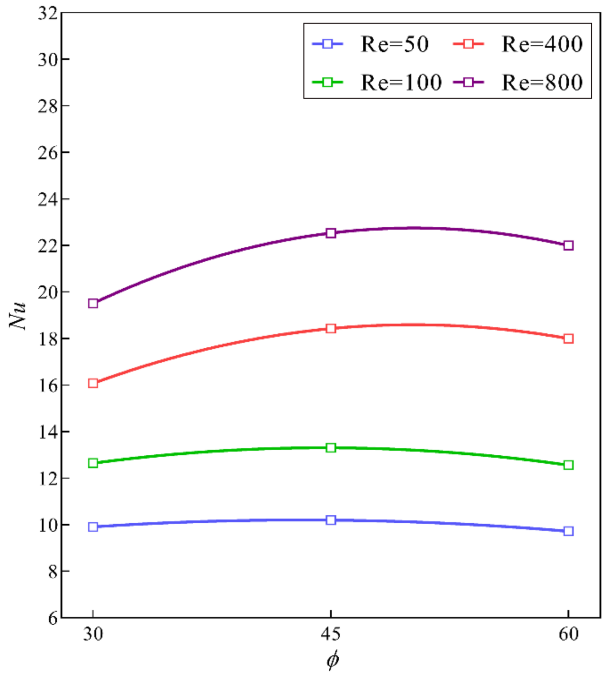

Figure 11. Effects of the change of ϕ on Nu, for a perforated plate-fin channel with $\alpha = 10$ and $\Psi = 90°$.

In Figures 10 and 11, the effects of the change of ϕ on f, and Nu are depicted respectively. Figure 10 shows that f increases with ϕ, with a gradual slope, for all values of Re. Figure 11 shows that Nu gradually increases as ϕ approaches 45°, then it decreases slowly as it approaches 60°. The decrease in Nu with an angle exceeding 45° may be explained by the fact that as angle increases, the angled fin wall reduces the mixing of the fluid resulting from flow transpiration, and thereby eliminates the gain caused by the disruption of the boundary layer. In Figure 12, the changes in the channel's area goodness factor are shown as a result of changing ϕ. A very small variation in the area goodness factor is observed over the whole range of ϕ. Based on the results, it is evident that with increasing corrugation angle from 30° to 45°, the 3-D trapezoid-shaped perforated plate-fin channel's performance improves; however, as the angle increases more, performance begins to decline.

3.2.2. Effect of the cross-section aspect ratio ($\alpha = H/S_{avg}$)

Figure 13 shows the flow cross-section location markers at different points along the axial length of the one period of the 3-D perforated plate-fin channel including trapezoid-shaped fins of rectangular cross sections. The effects of cross-section aspect ratio on flow streamlines as well as temperature distribution at different axial locations of a 3-D perforated converging-diverging plate-fin channel with $\phi = 45°$, $\Psi = 90°$ are respectively

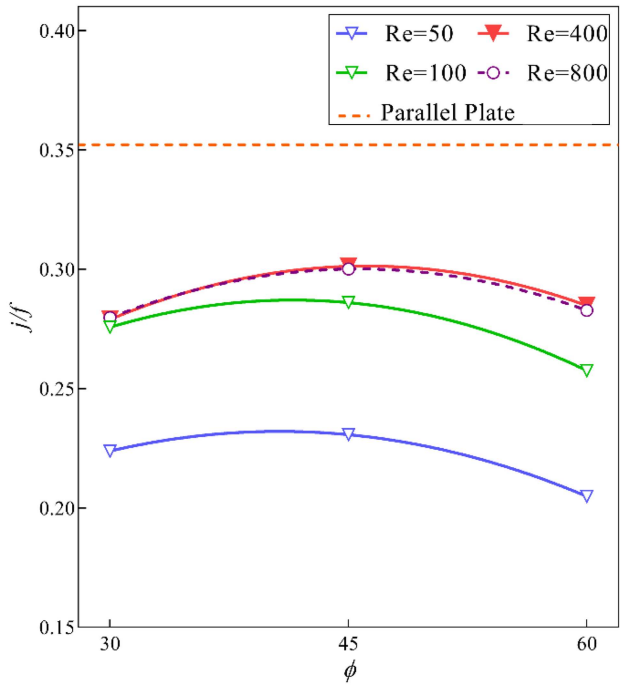

Figure 12. Effects of the change of ϕ on j/f, for a perforated plate-fin channel with $\alpha = 10$ and $\Psi = 90°$.

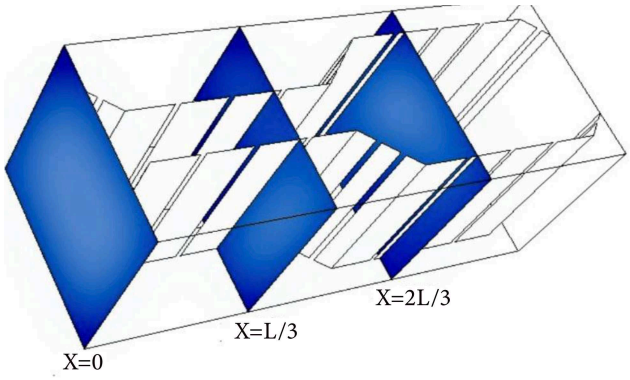

Figure 13. Different selected axial locations of the perforated plate-fin channel including trapezoid-shaped fins of rectangular cross sections.

demonstrated in Figures 14 and 15 for $Re = 400$. By increasing fin height or the cross-section aspect ratio, $\alpha = 1 \rightarrow 4$, A spatial coverage and strength increase are observed for counter-rotating vortices (Figure 14), resulting in greater convective mixing and in any case, the high mixing of the flow and the behavior of the vortex flow leads to an improved momentum and heat transfer (Figure 15).

Figures 16 and 17 respectively show the overall behavior of f and Nu for different values of α (1, 2, 4, and 10). Based on these figures, it is evident that f and Nu increase with increasing α, because the increased channel surface area and effective flow length (or residence time) lead to the symmetric pairs of counter-rotating helical swirls (Figure 14), that result in higher momentum and convective heat transfer. Figure 18 depicts the effects of changing α on the channel's area goodness factor. As can be seen from the results, the 3-D trapezoid-shaped perforated plate-fin channel's performance improves with increasing cross-section aspect ratio.

3.2.3. Effect of the cross-section inclination angle (Ψ) Figure 19 shows the flow cross-section location markers at different points along the axial length of the one period of the 3-D perforated plate-fin channel including trapezoid-shaped fins of trapezoidal cross sections. The effects of cross-section inclination angle on flow streamlines as well as temperature distribution at different axial locations of a 3-D perforated converging-diverging plate-fin channel with $\alpha = 45°$, $\alpha = 2$ are respectively demonstrated in Figures 20 and 21 for $Re = 400$. By changing the cross-section inclination angle from $\Psi = 90°$ to $\Psi = 76.60°$ (rectangular to trapezoidal cross section), the symmetric pairs of counter-rotating helical swirls are converted into one stronger counter-rotating vortex near the large bases of the trapezoidal cross sections on each side of the fin (Figure 20), resulting in higher convective mixing and improved momentum and heat transfer (Figure 21).

Figures 22 and 23 respectively show the general behavior of f and Nu for different values of Ψ (90°, 85.46°, 80.98°, and 76.60°). From these figures, it is apparent that when Ψ is changed from 90° to 76.60°, f decreases and Nu increases; Because the increase in fin surface area leads to increased convective heat transfer and Nusselt number; however, the increase in perforation surface area reduces pressure drop and f; The latter result is an unusual and highly desirable feature. Based on the results, when Ψ is changed from 90° to 76.60°, at $Re = 200$, the friction factor decreases $\sim 1.3\%$, and the area goodness factor increases $\sim 8.2\%$.

Figure 24 depicts the effects of changing Ψ on the channel's area goodness factor. The results indicate that the performance of the 3-D trapezoid-shaped perforated plate-fin duct improves by changing Ψ from 90° to 76.60°.

4. Conclusions

The numerical results presented in this paper provide an insightful analysis of forced convection of periodically fully developed incompressible airflow in 3-D perforated trapezoid-shaped symmetric plate-fin channels, having low Reynolds numbers ($10 \leq Re \leq 1000$). The results of the study are as follows:

- In the diverging region of the duct, wall transpiration, boundary layer disruption, and flow mixing are enhanced by the perforated fin surfaces, which reduce stagnation and recirculation zones and improve heat transfer;

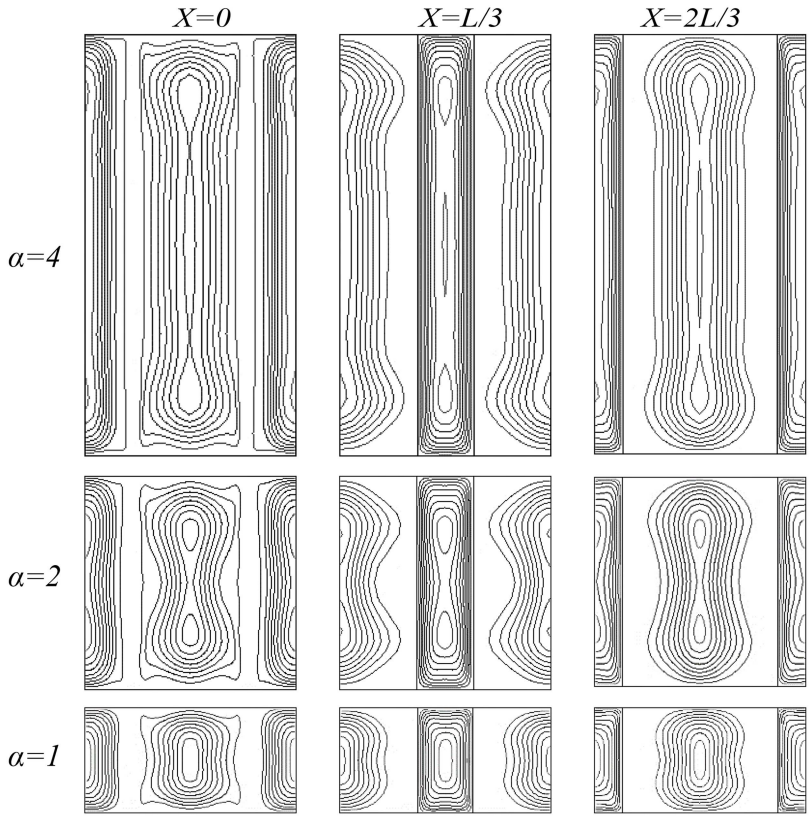

Figure 14. Effect of the cross-section aspect ratio (α) on flow streamlines at different axial locations of a perforated plate-fin channel with $\phi = 45°$, and $\Psi = 90°$ at $Re = 400$.

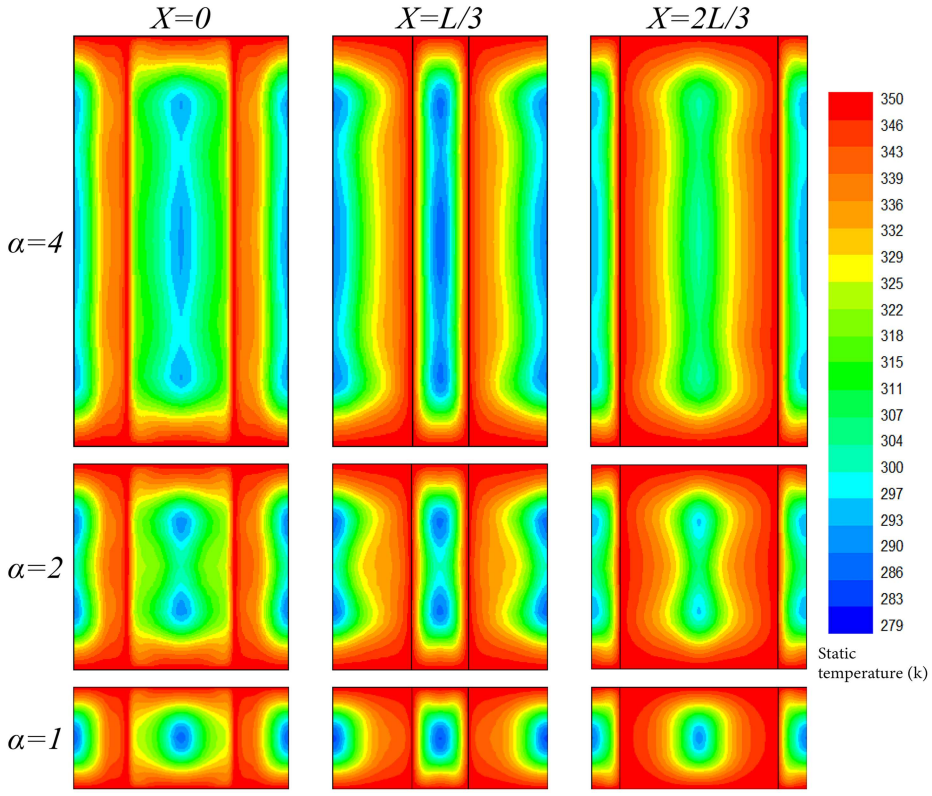

Figure 15. Effect of the cross-section aspect ratio (α) on temperature distribution at different axial locations of a perforated plate-fin channel with $\phi = 45°$, $\Psi = 90°$ at $Re = 400$.

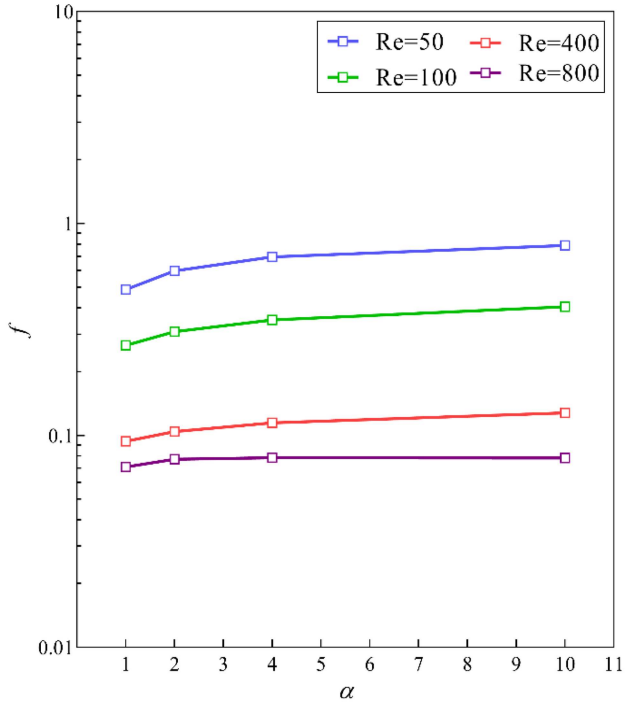

Figure 16. Effects of the change of α on f, for a perforated plate-fin channel with $\phi = 45°$and $\Psi = 90°$.

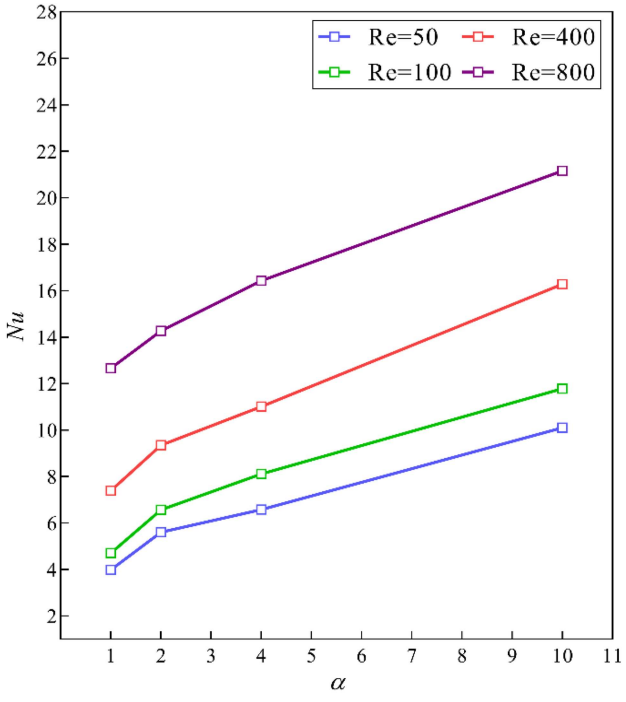

Figure 17. Effects of the change of α on Nu, for a perforated plate-fin channel with $\phi = 45°$and $\Psi = 90°$.

- Increasing heat transfer is associated with a reduction in friction losses, in comparison to the non-perforated channel, resulting in a significant decrease in frontal area (calculated by the area goodness factor (j/f)). For example, for a perforated case with $\phi = 45°$, $\alpha = 10$, and $\Psi = 90°$ at $Re = 200$, versus the non-perforated channel, the friction factor decreases $\sim 9\%$, and the area goodness factor increases $\sim 61\%$;
- When the corrugation angle (ϕ) varies from 30° to 60°, it is observed that f increases with Re for all the values of Re, with a gradual increase. Nu gradually increases as ϕ approaches 45°, then it decreases slowly as it approaches 60°. The decrease in Nu with an angle exceeding 45°may be explained by the fact that as angle increases, the angled fin wall reduces the mixing of the fluid resulting from flow transpiration, and thereby eliminates the gain caused by the disruption of the boundary

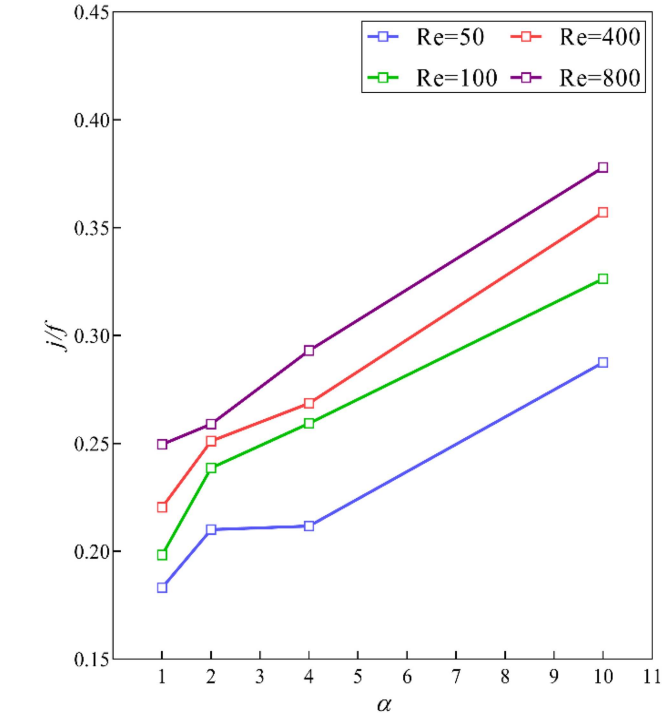

Figure 18. Effects of the change of α on j/f, for a perforated plate-fin channel with $\phi = 45°$and $\Psi = 90°$.

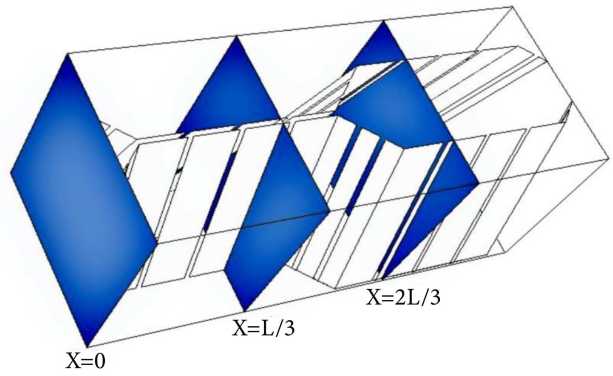

Figure 19. Different selected axial locations of the perforated plate-fin channel including trapezoid-shaped fins of trapezoidal cross sections.

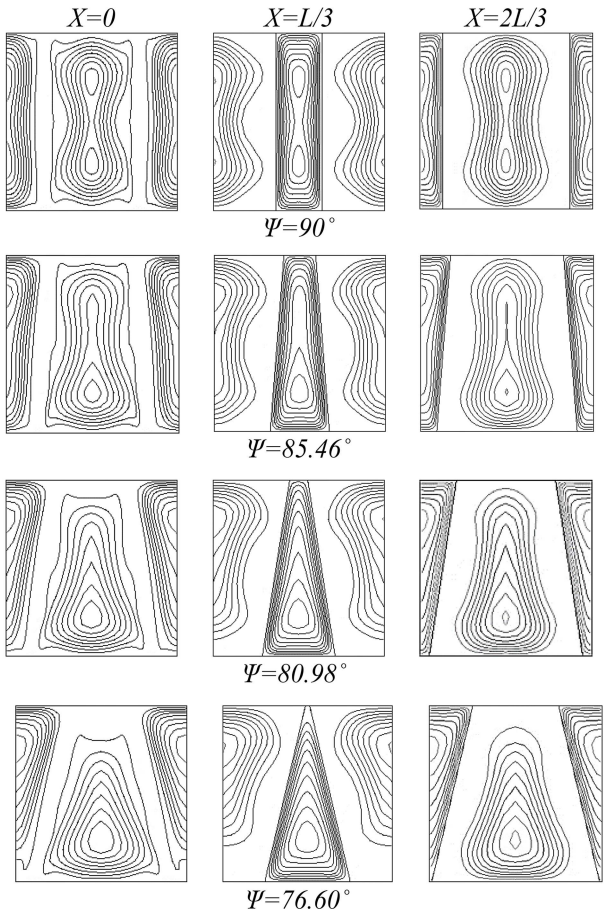

Figure 20. Effect of the cross-section inclination angle (Ψ) on flow streamlines at different axial locations of a perforated plate-fin channel with $\phi = 45°$, $\alpha = 2$ at $Re = 400$.

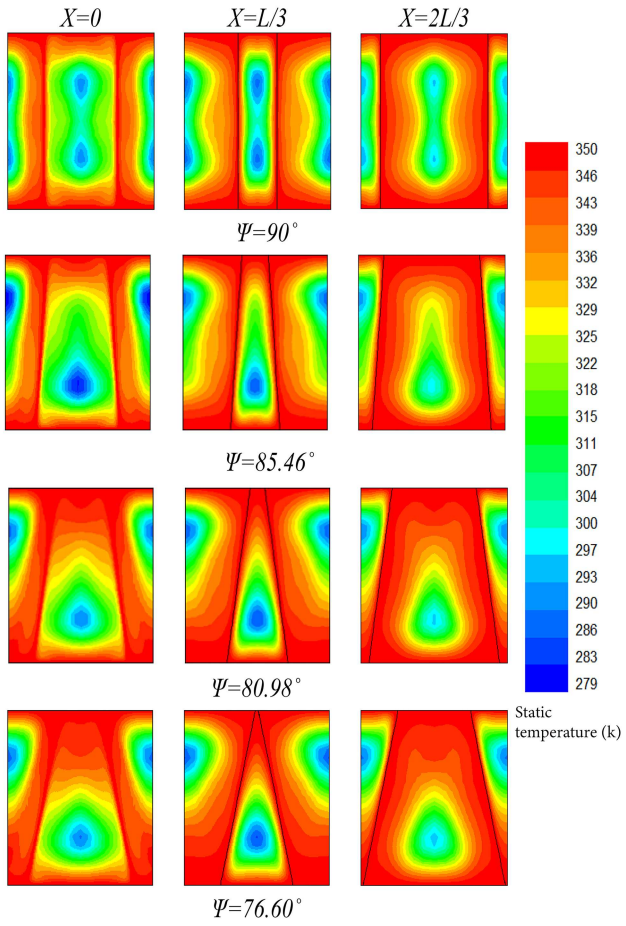

Figure 21. Effect of the cross-section inclination angle (Ψ) on temperature distribution at different axial locations of a perforated plate-fin channel with $\phi = 45°$, $\alpha = 2$ at $Re = 400$.

layer. With increasing corrugation angle from 30° to 45°, the 3-D trapezoid-shaped perforated plate-fin channel's performance improves; however, as the angle increases more, performance begins to decline;

- With increasing the cross-section aspect ratio (α) from 1 to 10, both f and Nu increase, because the increased channel surface area and effective flow length (or residence time) lead to the symmetric pairs of counter-rotating helical swirls that provide higher momentum and convective heat transfer. As well, the 3-D trapezoid-shaped perforated plate-fin channel's performance improves with increasing cross-section aspect ratio;
- When the cross-section inclination angle (Ψ) is changed from 90° to 76.60° (rectangular to trapezoidal cross section), the symmetric pairs of counter-rotating helical swirls are converted into one stronger counter-rotating vortex near the large bases of the trapezoidal cross sections on each side of the fin, resulting in higher convective mixing and improved momentum and heat transfer. By changing Ψ from 90° to 76.60°, f decreases and Nu increases;

Because the increase in fin surface area leads to increased convective heat transfer and Nusselt number; however, the increase in perforation surface area reduces pressure drop and f; The latter result is an unusual and highly desirable feature. Based on the results, when Ψ is changed from 90° to 76.60°, at $Re = 200$, the friction factor decreases $\sim 1.3\%$, and the area goodness factor increases $\sim 8.2\%$.

Nomenclature

A_c	Cross section flow area of a duct, (m^2)
D_h	Hydraulic diameter, (m)
f	Fanning friction factor
j	Colburn factor
k	Thermal conductivity of fluid, (W/m.K)
L	Pitch of fin waviness, (m)
$\dot{m}$	Mass flow rate, (kg/s)
Nu	Average Nusselt number
Nu_x	Local Nusselt number

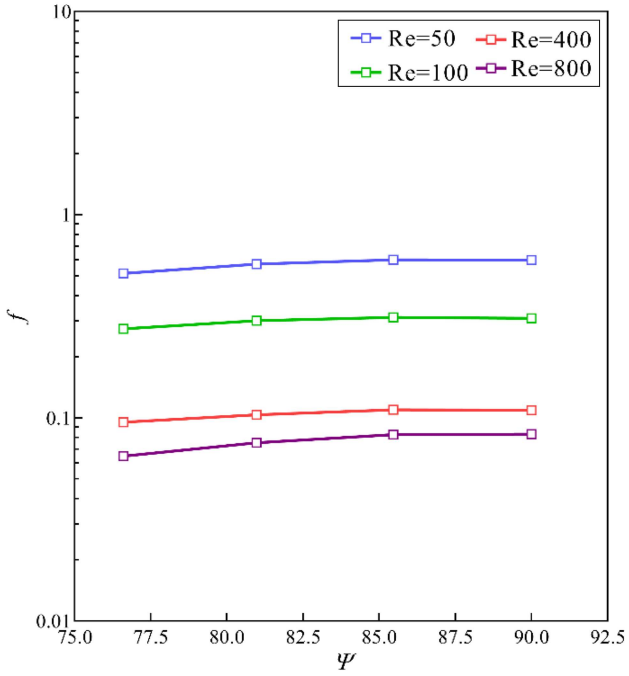

Figure 22. Effects of the change of Ψ on f, for a perforated plate-fin channel with $\phi = 45°$and $\alpha = 2$.

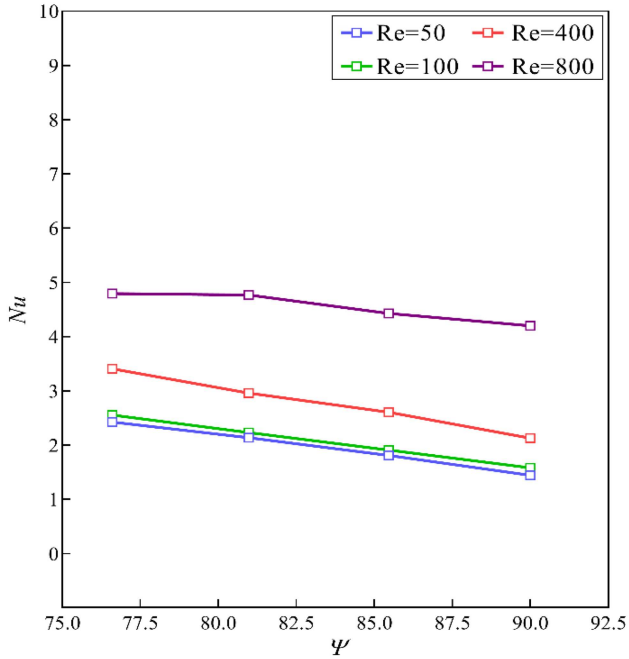

Figure 23. Effects of the change of Ψ on Nu, for a perforated plate-fin channel with $\phi = 45°$and $\alpha = 2$.

Pr	Prandtl number
P	Pressure, (Pa)
q''	Heat flux, (W/m^2)
Re	Reynolds number
S	Fin spacing, (m)
T	Temperature, (K)

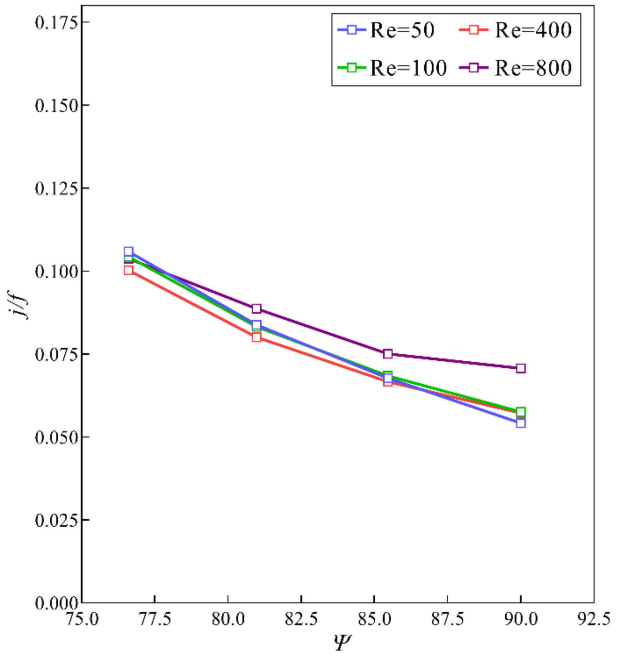

Figure 24. Effects of the change of Ψ on j/f, for a perforated plate-fin channel with $\phi = 45°$and $\alpha = 2$.

T_b	Bulk temperature, (K)
$T_{b,x}$	Local bulk temperature, (K)
T_w	Wall temperature, (K)
$T_{w,x}$	Local wall temperature, (K)
u, v	Velocity components, (m/s)
U_b	Bulk horizontal velocity, (m/s)
x, y	Cartesian coordinates

Greek letters

a	Cross-section aspect ratio
α	Thermal diffusivity, (m^2/s)
$\varepsilon_h{}^d$	Discretization error
μ	Dynamic viscosity, (kg/m.s)
υ	Kinematic viscosity, (m^2/s)
ρ	Density, (kg/m^3)
τ	Shear tress, (Pa)
Φ	Richardson solution
ϕ	Corrugation angle
φ_h	Finest mesh solution
Ψ	Cross-section inclination angle

Subscripts

b	Bulk value
c	Cross-section
w	Wall

References

1. Kays, W.M. and London, A.L., *Compact Heat Exchangers*, McGraw-Hill, New York (1984).
2. Bergles, A.E. "Techniques to enhance heat transfer", In *Handbook of Heat Transfer*, W.M. Rohsenow, J.P. Hartnett, and Y.I. Cho, Ed., Chapter 11, McGraw-Hill, New York (1998).
3. Shah, R.K. and Sekulic, D.P., *Fundamentals of Heat Exchanger Design*, John Wiley and Sons, New York (2003).
4. Manglik, R.M. "Heat transfer enhancement", In *Heat Transfer Handbook*, A. Bejan, and A.D. Kraus, Ed., Chapter 14, Wiley, Hoboken, NJ (2003).
5. Webb, R.L. and Kim, N.H. "Principles of enhanced heat transfer", Taylor and Francis, Boca Raton, FL (2005).
6. London, A.L. "A Brief history of compact heat exchanger technology", In *Compact Heat Exchangers - History, Technological Advancement and Mechanical Design Problems*, pp. 1–4, ASME, New York (1980).
7. Manglik, R.M. and Bergles, A.E. "The thermal hydraulic design of the rectangular offset strip-fin compact heat exchanger", *Compact Heat Exchangers: A Festschrift for A.L. London*, pp. 123–149 (1990).
8. Bergles, A.E., Jensen, M.K., Sommerscales, E.F.C., et al. "Literature review of heat transfer enhancement technology for heat exchangers in gas-fired applications", Report No. GRI 91–0146 (1991).
9. Manglik, R.M. and Bergles, A.E. "Heat transfer and pressure drop correlations for the rectangular offset strip fin compact heat exchanger", *Experimental Thermal and Fluid Science*, **10**(2), pp. 171–180 (1995). DOI: 10.1016/0894-1777(94)00096-Q
10. Zhang, J., Kundu, J., and Manglik, R.M. "Effect of fin waviness and spacing on the lateral vortex structure and laminar heat transfer in wavy-plate-fin cores", *International Journal of Heat and Mass Transfer*, **47**(8-9), pp. 1719–1730 (2004). DOI: 10.1016/j.ijheatmasstransfer.2003.10.006
11. Manglik, R.M., Zhang, J., and Muley, A. "Low Reynolds number forced convection in three-dimensional wavy-plate-fin compact channels: fin density effects", *International Journal of Heat and Mass Transfer*, **48**(8), pp. 1439–1449 (2005). DOI: 10.1016/j.ijheatmasstransfer.2004.10.022
12. Shah, R.K. and London, A.L., *Laminar Flow Forced Convection in Ducts*, Academic Press, New York (1978).
13. Manglik, R.M. and Bergles, A.E. "Enhanced heat and mass transfer in the new millennium: A review of the 2001 literature", *Journal of Enhanced Heat Transfer*, **11**(2), pp. 87–118 (2004). DOI: 10.1615/JEnhHeatTransf.v11.i2.10
14. Shah, R.K. and Bhatti, M. "Laminar convective heat transfer in ducts", In *Handbook of Single-Phase Convective Heat Transfer*, S. Kakac, R.K. Shah, and W. Aung, Ed., pp. 3.1-3.137 (1987).
15. Sadasivam, R., Manglik, R.M., and Jog, M.A. "Fully developed forced convection through trapezoidal and hexagonal ducts", *International Journal of Heat and Mass Transfer*, **42**, pp. 4321–4331 (1999). DOI: 10.1016/S0017-9310(99)00091-5
16. Petkov, V.M., Zimparov, V.D., and Bergles, A.E. "Performance evaluation of ducts with non-circular shapes: Laminar fully developed flow and constant wall temperature", *International Journal of Thermal Sciences*, **79**, pp. 220–228 (2014). DOI: 10.1016/j.ijthermalsci.2013.12.005
17. Reis, M.C., Sphaier, L.A., Alves, L.S., et al. "Approximate analytical methodology for calculating friction factors in flow through polygonal cross section ducts", *Journal of the Brazilian Society of Mechanical Sciences and Engineering*, **40**(76) (2018). DOI: 10.1007/s40430-018-1019-6
18. Abed, AlKareem, S.S., Khudheyer, A.F., and Mustafa, F.F. "Numerical investigation of turbulent air Flow convective heat transfer through a trapezoidal duct", *Journal of Mechanical Engineering Research and Developments*, **43**(7), pp. 100–108 (2020).
19. Fujii, M., Seshimo, Y., and Yamanaka, G. "Heat transfer and pressure drop of perforated surface heat exchanger with passage enlargement and contraction", *International Journal of Heat and Mass Transfer*, **31**(1), pp. 135–142 (1988). DOI: 10.1016/0017-9310(88)90230-x
20. Fujii, M., Seshimo, Y.U., Ueno, S., et al. "Forced air heat sink with new enhanced fins", *Heat Transfer, Japanese Research*, **18**(6), pp. 53–65 (1989).
21. Ji, T.H., Kim, S.Y., and Hyun, J.M. "Pressure drop and heat transfer correlations for triangular folded fin heat sinks", *IEEE Transactions on Components and Packaging Technologies*, **30**, pp. 3–8 (2007). DOI: 10.1109/TCAPT.2006.885943
22. Ganorkar, A.B. and Kriplani, V.M. "Experimental study of heat transfer rate by using lateral perforated fins in a rectangular channel", *MIT International Journal of Mechanical Engineering*, **2**(2), pp. 91–96 (2012).
23. Shahdad, I. and Fazelpour, F. "Numerical analysis of the surface and geometry of plate fin heat exchangers for increasing heat transfer rate", *International Journal of Energy and Environmental Engineering*, **9**, pp. 155–167 (2018). DOI: 10.1007/s40095-018-0270-z
24. Mohammad, M., Talukder, M.P.H., Rahman, K.A., et al. "Experimental investigation on the effect of different perforation geometry of vertical fins under forced convection heat transfer", *International Conference on Mechanical Engineering and Renewable Energy*, Chittagong, Bangladesh (2019).
25. Kumar, B., Patil, A.K., Kumar, M., et al. "Performance enhancement by perforated twisted tape tube insert with single and double V cuts in heat exchanger tube", *Heat Transfer Research*, **51**(5), pp. 395–406 (2020). DOI: 10.1615/HeatTransRes.2019029789

26. Noorbakhsh, M., Zaboli, M. and Mousavi, S.S. "Numerical evaluation of the effect of using twisted tapes as turbulator with various geometries in both sides of a double pipe heat exchanger", *Journal of Thermal Analysis and Calorimetr*, **140**(1), pp. 1341–1353 (2020). DOI: 10.1007/s10973-019-08509-w

27. Pradeep, H., Pramoda, B.S., Shivakumar, H.S., et al. "Design and analysis on effects of different fin perforations", *International Journal of Future Generation Communication and Networking*, **13**(3), pp. 1141–1152 (2020).

28. Srivastava, G.P., Patil, A.K., and Kumar, M. "Parametric effect of diverging perforated cones on the thermo-hydraulic performance of a heat exchanger tube", *Heat and Mass Transfer*, **57**, pp. 1425–1437 (2021). DOI: 10.1007/s00231-021-03035-8

29. Rauber, W.K., Silva, U.F., Vaz Jr., M., et al. "Investigation of the effects of fin perforations on the thermal-hydraulic performance of Plate-Finned heat exchangers", *International Journal of Heat and Mass Transfer*, **187**, (2022). DOI: 10.1016/j.ijheatmasstransfer.2022.122561

30. Piradl, M. and Pesteei, S.M. "Numerical study of heat transfer of laminar air flow in perforated trapezoidal corrugated plate-fin ducts", *Journal of Mechanical Engineering Science*, **236**(6), pp. 3216–3229 (2022). DOI: 10.1177/09544062211034544

31. Chen, Y., Chen, H., Zeng, H., et al. "Structural optimization design of sinusoidal wavy plate fin heat sink with crosscut by Bayesian optimization", *Applied Thermal Engineering*, **213**, (2022). DOI: 10.1016/j.applthermaleng.2022.118755

32. Towsyfyan, H., Freegah, B., Hussain, A.A., et al. "Novel design to enhance the thermal performance of plate-fin heat sinks based on CFD and artificial neural networks", *Applied Thermal Engineering*, **219** (2023). DOI: 10.1016/j.applthermaleng.2022.119408

33. Eiamsa-ard, S., Phila, A., Wongcharee, K., et al. "Thermal evaluation of flow channels with perforated-baffles", *Energy Reports*, **9**(3), pp. 525–532 (2023). DOI: 10.1016/j.egyr.2023.01.064

34. Ferziger, J.H. and Peric, M., *Computational Methods for Fluid Dynamics*, Springer, 3rd Edition (2002).

35. Richardson, L.F. "The approximate arithmetical solution by finite differences of physical problems including differential equations, with an application to the stresses in a masonry dam", *Philosophical Transactions of the Royal Society A*, **210**(459-470), pp. 307–357 (1911). DOI: 10.1098/rsta.1911.0009

36. Richardson, L.F. and Gaunt, J.A. "The deferred approach to the limit", *Philosophical Transactions of the Royal Society A.*, **226**(636–646), pp. 299–349 (1927). DOI: 10.1098/rsta.1927.0008

Biographies

Morteza Piradl received his MSc in energy conversion in 2011, from Urmia University, Iran. He is currently a PhD candidate at the Department of Mechanical Engineering, Urmia University, Iran. His research areas include fluid flow and heat transfer in compact heat exchangers, parallel programing, and cooling and heating technologies.

Seyed Mehdi Pesteei received his master's degree in mechanical engineering (energy conversion) in 1989, from Dokuz- Eylul University, Izmir, Turkey. In 1990, he worked as a faculty member with the rank of educational instructor in the Mechanical Engineering Department of Urmia University. He received his PhD degree in 2002 in the field of mechanical engineering and energy conversion from the Indian Institute of Technology-Delhi (I.I.T. Delhi-India). Currently, he is working as an associate professor in the Department of Mechanics, Urmia University. His research activities include, convection heat transfer, air conditioning, cooling, and heating systems, design of heat exchangers and solar collectors. His C.V. web page: http://facultystaff.urmia.ac.ir/sm.pesteei.